Investigation of the Conformational States of Wzz and the Wzz·O-Antigen Complex under Near-Physiological Conditions†

Kuo-Hsiang Tang,‡,§,|| Hongjie Guo,‡,|| Wen Yi,‡ Ming-Daw Tsai,‡,§ and Peng George Wang*,‡,⊥

Departments of Chemistry and Biochemistry, The Ohio State University, Columbus, Ohio 43210, Genomics Research Center, Academia Sinica, Taiwan, R.O.C., and The State Key Laboratory of Microbial Technology, School of Life Science, Shandong University, Jinan, Shandong 250100, P.R.C.

Received June 14, 2007; Revised Manuscript Received August 4, 2007

ABSTRACT: Chain length determinant protein (Wzz) has been postulated to terminate the polymerization and regulate the chain length of the O-polysaccharide (O-antigen), an important component for constructing lipopolysaccharide (LPS) in the outer membrane of Gram-negative bacteria. The investigation to understand the mechanism of Wzz has been largely slowed down due to lack of structural information. In this report, we have applied small-angle X-ray scattering (SAXS) to study the conformational state and molecular properties of Wzz and the Wzz·O-antigen complex under near-physiological conditions. No concentration-dependent aggregation or structural changes, but repulsive intermolecular interactions between Wzz molecules, are suggested in the concentration series studies. The SAXS studies suggest that Wzz protein appears to be elongated and exists as a tetramer in solution. The reconstructed model built from SAXS data indicates that the middle regime of Wzz, most likely representing the periplasmic domain, contributes to the Wzz oligomerization, which has been proposed to be correlated to the function of Wzz. The immunoblotting analyses also demonstrate that the putative coiled-coil region in the periplasmic region contributes to the oligomerization. Further, the SAXS data corresponding to Wzz and the Wzz·O-antigen complex indicate an apparent substrate (O-antigen)-induced conformational change, consistent with previous circular dichroism studies. Our finding may shed light on the biological mechanism of Wzz as a chain length determinant of O-antigen.

Lipopolysaccharide (LPS) constitutes the major component of the outer leaflet of the outer membrane in Gram-negative bacteria (*1*). It mainly contributes to the cell structural integrity and pathogenicity. LPS consists of three structural parts: (i) lipid A, glucosamine-based phospholipids, which is the major component to elicit innate immune response; (ii) core oligosaccharide; and (iii) O-polysaccharide (O-antigen) that contains multiple copies of an oligosaccharide unit (O-repeating unit). O-antigen plays an important role in the bacterial resistance to serum-mediated killing, phagocytosis, and killing by cationic peptides (*2, 3*). The working model for the biosynthesis of heteropolymeric O-antigens is described as Wzy-dependent pathway (Figure 1) (*1*). This pathway starts with the sequential assembly of O-repeating unit at the cytoplasmic face of the inner membrane. These intermediates are then translocated by O-antigen flippase Wzx to the periplasm (*4*−*6*). In the periplasm, they serve as substrates for polymerization process dependent on O-antigen polymerase Wzy (*7*−*9*). Chain length determinant protein Wzz is proposed to terminate the polymerization and regulate the chain length of the polysaccharide. O-antigen is then linked to the preformed lipid-A-core structure by WaaL ligase. The final translocation of the entire LPS molecule from the periplasm to the cell surface was recently proposed to be mediated by an outer membrane protein complex Imp/RlpB (*10*).

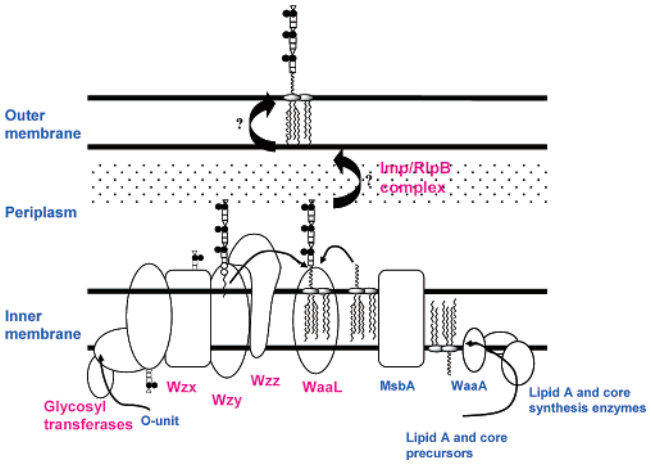

FIGURE 1: Biosynthesis of lipopolysaccharides in Gram-negative bacteria. In the Wzy-dependent pathway (see introduction), Wzz is hypothesized to terminate the polymerization and to regulate the chain length of the polysaccharide.

† This work was supported by National Institutes of Health Grant RO1 AI44040 (to P.G.W.) and National Science Council Grant 98-3112-B (to M.-D.T.). K.-H.T. was partially supported by an Academia Sinica Postdoctoral Fellowship. P.G.W. acknowledges the support from an endowed professorship of Ohio Eminent Scholar on macromolecular structure and function in the Department of Biochemistry at The Ohio State University.

* Corresponding author. Phone: (614) 292-9884. Fax: (614) 688-3106. E-mail: wang.892@osu.edu.

‡ The Ohio State University.

§ Academia Sinica.

|| The first two authors contributed equally to the work.

⊥ Shandong University.

10.1021/bi701181r CCC: $37.00
Published on Web 09/27/2007

Genetic study has shown that Wzz dictates the strain-specific modal distribution of O-antigen chain length. The wzz gene homologues are present in all Wzy-dependent O-antigen biosynthetic systems. Several models have been proposed to explain the control of Wzz over the modality of the polysaccharides. Bastin et al. (*11*) suggested that Wzz functions as a molecular timer that modulates the Wzy activity between two states favoring either polymerization or termination by transferring to the ligase WaaL. Morona et al. (*12*) have suggested that Wzz serves as a molecular chaperone to recruit a protein complex consisting of Wzy, WaaL, and nascent polysaccharide chains. The specific modality is conferred by different kinetics resulting from different ratios of Wzy to WaaL. Currently there is no definitive biochemical evidence for either model. Recently, we developed an efficient expression system to obtain large quantity of homogeneous Wzz (*13*). Using circular dichroism (CD), we have shown that Wzz interacts with O-antigens, and that different O-antigen substrates produce similar binding affinity with the same Wzz. This finding provides an additional piece of biochemical information for understanding Wzz function.

Wzz primary sequences are very well conserved, as are the predicted membrane topologies. Wzz proteins are grouped in the "polysaccharide co-polymerases" (PCP) superfamily, members of which are involved in the chain length regulation of a variety of polysaccharides including O-antigens, capsular polysaccharides, and exopolysaccharides. Wzz proteins have a characteristic membrane topology: two transmembrane helices are located near the amino- and carboxyl-terminals, respectively. Until recently, no structural information was available for the proteins in this family. Collins et al. (*14*, *15*) reported the three-dimensional structure of Wzc, a homologue of Wzz involved in chain length regulation of group 1 capsular polysaccharides, but distinguished from Wzz by possession of a C-terminal domain harboring ATP-binding motif and tyrosine-rich residues. The structure was derived from single-particle analysis of negatively stained samples in cryo-electron microscope (cryo-EM) and resolved at 14 Å. It forms a tetramer with C4 rotational symmetry. Since Wzc and Wzz share similar membrane topology, it is temping to speculate that they have similar structure and function.

To date, there is still no structural information for Wzz, which significantly slows down the interpretation of Wzz mechanisms. In the absence of atomic resolution structures acquired by X-ray crystallography or NMR spectroscopy, small-angle X-ray scattering[1] (SAXS) can provide global low-resolution structural information for many macromolecules and complexes under near-physiological conditions (*16*), thereby the structural and functional studies can be appropriately compared. In this paper, we report the SAXS and biochemical studies of Wzz to provide structural insights and molecular properties of Wzz and the Wzz·O-antigen complex, and the studies suggest that oligomerization of Wzz, which is essential for determining the chain length of polysaccharide, is mediated by the periplasmic domain with the predicted coiled-coil region. The O-antigen-induced conformational change is indicated by SAXS studies. Finally, we discuss our studies with the current working hypotheses of the mechanism of action of Wzz.

[1] Abbreviations: DDM, dodecyl maltoside; SAXS, small-angle x-ray scattering.

MATERIALS AND METHODS

Sample Preparation. n-Dodecyl-β-D-maltoside (DDM) (MW, 510.6) was purchased from Sigma, anti-GST and anti-Myc antibodies were from Invitrogen (Carlsbad, CA), and *Escherichia coli* O86:H2 Wzz and O-antigen (10−18 O units) were purified as described previously (*13*). All of the Wzz described in this report are the DDM-bound Wzz proteins. DDM-bound Wzz was prepared in 20 mM Tris-HCl (pH 8.0), 0.01−0.05% (v/w) of DDM, and with or without NaCl. The protein concentration was estimated by Bradford protein assay.

Small-Angle X-ray Scattering (SAXS). SAXS was conducted at BL 4-2 of the Stanford Synchrotron Radiation Laboratory (SSRL), and at BioCAT 18-ID of the Advanced Photon Sources (APS). At BL 4-2 data were collected at 8980 eV, corresponding to an X-ray wavelength (λ) of 1.38 Å. The scattering curves were measured at different sample-to-detector distances and covered the momentum transfer range 0.008 $Å^{-1} < Q < 0.54$ $Å^{-1}$ (where $Q = 4\pi \sin \theta/\lambda$, 2θ is the scattering angle). The Lexan sample cells (15 μL) with thin mica windows were maintained at a constant temperature of 20 ± 0.5 °C during the measurements. The scattering patterns were collected in ten sequential 30 s frames using a MarCCD 165 area detector (Mar, IL). The images were processed with the program MarParse developed by BL 4-2. At BioCAT 18-ID data were collected with an 160 × 80 mm^2 Aviex CCD detector (Aviex, IL). The X-ray wavelength was 1.033 Å (12 keV). A sample-to-detector distance of 1860 mm corresponded to 0.007 $Å^{-1}$ to 0.507 $Å^{-1}$ in Q. The scattering curves were collected as 10 exposures of 1 s with the full beam. The sample volume was 120 μL, and the temperature was kept at 20 ± 0.2 °C. During exposures the samples were flowing unidirectionally as a rate of 1.0 μL/s through the cell to reduce radiation damage. The radiation damage was tested by comparing subsequent exposures of the same sample, and only the data without the signs of radiation damage were analyzed. Exposures from sample and buffer were alternated to minimize the possible effects of drift in any experimental parameter. The data processing and evaluation were performed using the IgorPro package (WaveMetrics, Inc.) enhanced with BioCAT-developed custom macros.

Determination of the Molecular Mass of the DDM-Bound Wzz by SAXS. Two reference proteins were used to evaluate the molecular mass of DDM-bound Wzz protein: one is the mammalian DNA polymerase β (Pol β), a 38.4 kDa monomeric protein with 335 amino acid residues. Pol β was chosen because it has similar molecular mass to the monomer of Wzz, and is rather stable, frequently used in our SAXS measurements, no concentration-dependent oligomerization or aggregation, and exists as an elongated shape as the DDM-bound Wzz (described in Results and Discussion). The other is bovine serum albumin (BSA, a 66.4 kDa monomeric protein), which is one of the most common standards (*17*) for estimating the molecular mass of the studied protein. The forward scattering intensity for the DDM-bound Wzz protein can be expressed in eq 1 (*18*),

$$I(0) = Kc(N_{Wzz}\Delta\rho_{Wzz}M_{Wzz} + N_{DDM}\Delta\rho_{DDM}M_{DDM})^2 \quad (1)$$

where the molecular mass for Wzz protein and DDM is M_{Wzz} and M_{DDM}, respectively. N_{Wzz} (or N_{DDM}) is number of Wzz (or DDM) molecules in the DDM-bound Wzz complex, and c is the concentration of DDM-bound Wzz protein. The average electron density contrast for Wzz is $\Delta\rho_{Wzz}$, where $\Delta\rho_{Wzz} = \rho_{Wzz} - \rho_{buffer}$, and for DDM-micelle is $\Delta\rho_{micelle}$, where $\Delta\rho_{micelle} = \rho_{micelle} - \rho_{buffer}$. The average electron density ($\rho_{electron}$, e/Å^3) of protein, DDM, and solvent (buffer) molecule is ~0.442 (*19*), 0.398 (*20*), and 0.334, respectively. The proportionality constant K depends on experimental parameters, which are held constant throughout the measurements and can be determined by comparison with a molecular weight standard.

By comparing the extrapolated forward scattering intensity $I(0)$ of DDM-bound Wzz with that of the standard protein (Pol β and BSA) in SAXS measurements, the molecular mass of the DDM-bound Wzz protein is estimated using the eq 1 to be ~256 kDa, similar to the molecular mass determined by size-exclusion chromatography, ~224 kDa (*13*). The experimental molecular mass of the micelle-bound Wzz is consistent with a tetrameric Wzz protein with 41 kDa (363 residues, including a C-terminus His-tag as part of pBAD/Myc-His vector (*13*)) per monomer. The molecular mass of the DDM-bound micelle is ~80 kDa, similar to the reported value (~60−75 kDa) (*21*, *22*), and ~155−160 DDM molecules are bound to the tetrameric Wzz protein.

Data Analyses and Modeling. The forward scattering intensity ($I(0)$), the longest length of the particle (D_{max}), and the particle distance distribution function ($P(r)$) were obtained from the experimental SAXS data using the program GNOM (*23*). The value of radius of gyration (R_g) was determined using the Guinier approximation (*24*) with $Q_{max}R_g \leq 1.3$ as well as GNOM, which calculates R_g and $I(0)$ from the $P(r)$ function. Data points for $Q < 0.02$ Å^{-1}, which were affected by intermolecular interactions, were excluded from the data fit. The reported SAXS data were treated as monodisperse systems unless otherwise mentioned.

After processing the scattering data with GNOM, the modeling program GASBOR (*25*), which represents the particle as a collection of dummy residues, was used to determine the overall conformations of Wzz. The simulation starts with randomly positioned residues and utilizes simulated annealing to find a chain-compatible spatial distribution of dummy residues inside the search volume. Protein concentration series were measured for investigating the influence of interparticle interaction effects. The final scattering curve was obtained by merging the small angle data (Q-range from 0.02 to 0.15 Å^{-1}) of the low concentration sample (0.5 mg/mL) with the data in the high angle region (Q-range from 0.10 to 0.50 Å^{-1}) of the high concentration data (10 mg/mL) with PRIMUS (*26*), to eliminate interparticle interaction effects in the low angle region.

The model was first constructed without symmetrical constraint being applied, and the common envelope exhibits an approximately 4-fold symmetry but resolution is relatively low. With the prior knowledge of DDM-bound Wzz protein being a tetramer obtained from previous studies (*13*) and this report, the P4-symmetry constraint was applied to increase the resolution of reconstructed model. And the model constructed without symmetry restriction is comparable with P4-symmetry constrained models reported herein. To evaluate the creditability and accuracy of the reconstructed model, we employed the program DAMAVER (*27*), which aligns all reconstructed models and removes outliers below a given cutoff volume, for setting up the criterion of the pairwise normalized spatial discrepancies (NSD). The *ab initio* models exceeding ⟨NSD⟩ (mean value of all pairs NSD) + 2Δ(NSD) (variation of NSD) were discarded, and the models except the outliners are shown in Figure S1 (Supporting Information). Due to the flexible N- and C-terminus of the reconstructed model, the total spread region is large and ⟨NSD⟩ = ~0.8. The most probable model of DDM-bound Wzz protein after DAMAVER processing is shown in Figure 5.

Interactions of Coiled-Coil Region with the Full-Length Wzz Protein. The middle part (residues 153−213) in the periplasmic domain of *E. coli* O86:H2 Wzz was predicted to have a moderate potential (18−38% probability) in forming coiled coils (*13*) using the program COILS (http://www.ch.embnet.org/software/COILS_form.html). The coiled-coil segment was cloned into pET-41 (Novagen, Madison, WI), and the coiled-coil segment was expressed as glutathione S-transferase (GST) fusion protein in *E. coli* BL21 (DE3). The recombinant protein was purified by GSH Sepharose affinity column. A GST-pulldown assay was carried out to study the interaction of the coiled-coil region with the full-length Wzz protein. The purified GST-coiled coil and the full-length Wzz protein were incubated with glutathione-Sepharose beads at room temperature for 2 h. In a similar fashion, the purified GST was incubated with the full-length Wzz protein and the glutathione-Sepharose beads as the negative control. The beads were washed 10 times with phosphate buffer saline (PBS). Bound proteins were eluted by 100 mM glutathione in PBS buffer and subjected to SDS−PAGE and immunoblotting. Anti-GST and anti-Myc antibodies were used to detect the coiled-coil-GST and the full-length Wzz protein.

RESULTS AND DISCUSSION

The Feasibility of Studying DDM-Bound Wzz by Small-Angle X-ray Scattering (SAXS). We first explore the possibility of applying SAXS to measure the association and conformation of transmembrane proteins in detergent micelle solutions. SAXS is widely applied to characterize the size and shape of water-soluble proteins and nucleic acids (*28*), but remains to be rather challenging to be applied in the studies of micelle-bound proteins and their complexes. The presence of detergent or micelle is required to make Wzz and other transmembrane proteins soluble by encapsulating the hydrophobic regions of the proteins while exposing their hydrophilic ends. But the presence of scattering intensity of detergents/micelles could represent a problem in some SAXS studies (described below). Further, the micelle-bound membrane proteins are not uncommon to be in unfolded conformations or/and aggregation forms, particularly in the high protein concentration so the reaction conditions need to be optimized for SAXS and other structural studies.

In SAXS measurements of the membrane-bound proteins, the scattering intensity is generated from the micelle-bound protein and unbound detergent micelles. The scattering

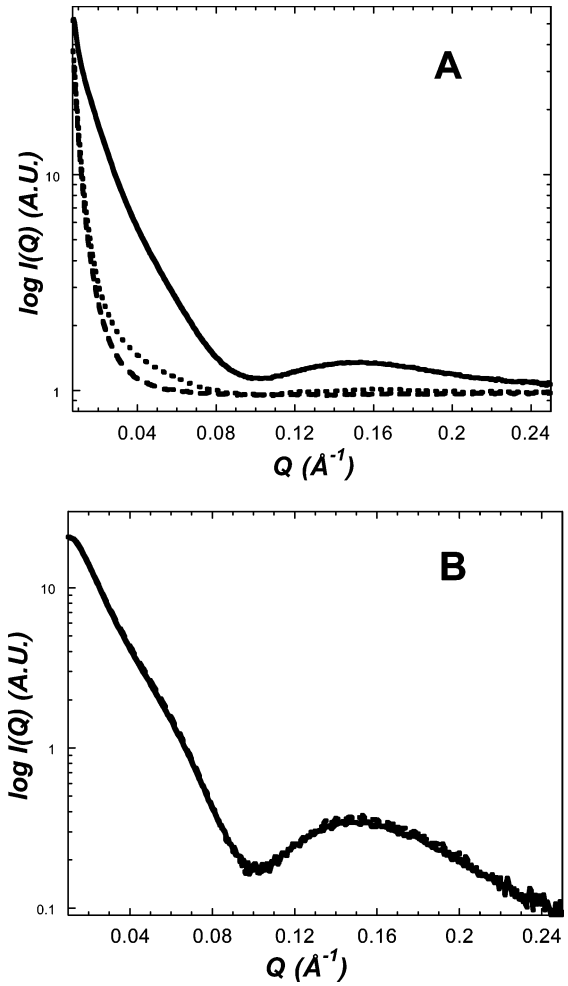

FIGURE 2: Experimental SAXS data for Wzz and DDM (solid line), and buffer with (dotted line) and without DDM (dashed line) included (A); and the SAXS patterns of DDM-bound Wzz with (solid line) or without (dashed line) DDM being subtracted (B). The sample preparation of SAXS measurements is described in Materials and Methods.

intensity of various detergents/micelles was investigated by SAXS (*19*, *29*, *30*). It was found that DDM, which is optimized for the stability and function of Wzz (*13*), has stronger scattering compared to most of the detergents (*20*). The high scattering intensity of DDM could complicate SAXS data analyses especially if high concentration of DDM is required for some membrane-bound proteins. To acquire the scattering intensity exclusively from the micelle-bound protein complex and not to overestimate the scattering of DDM-bound Wzz protein, dialysis against a buffer with known micelle concentration was performed in this report to ensure the fixed unbound micelle concentration. Our previous studies (*13*) indicated that Wzz is properly folded in 0.01−0.05% (w/v) (or 0.2−1.0 mM) DDM. Lower concentration of DDM required for Wzz can reduce the impact of stronger scattering intensity of DDM on the overall SAXS scattering. The actual effect of DDM micelles was investigated by SAXS, and the experimental data are shown in Figure 2. As predicted, similar values of R_g (the radius of gyration) and D_{max} (the longest length of the particle) were obtained with or without DDM in the buffer being subtracted in the scattering (Table 1). Additionally, although certain micelle-bound membrane proteins were shown to be larger in solution compared to the crystal form, due to the protein

Table 1: SAXS Data for Concentration-Series Studies of DDM-Bound Wzz Protein Obtained from Guinier Analyses and GNOM Fit

[DDM-bound Wzz] (mg/mL)	R_g		
	Guinier[a]	Guinier[b]	GNOM[b]
0.5	76.2 ± 0.2	75.8 ± 0.3	75.4 ± 0.2
1	75.2 ± 0.2	76.6 ± 0.4	75.2 ± 0.2
2	73.9 ± 0.2	73.6 ± 0.3	73.2 ± 0.3
4	70.1 ± 0.3	71.9 ± 0.2	69.4 ± 0.4
10	66.1 ± 0.1	65.4 + 0.1	65.1 ± 0.1

[a] Only buffer scattering was subtracted from the scattering intensity of DDM-bound Wzz protein. [b] Buffer and DDM signals were subtracted from the scattering intensity of DDM-bound Wzz.

molecule being surrounded by the detergent molecules (*30*), no differences were observed in the reconstructed models of DDM-bound Wzz protein with or without consideration of micelles. Lack of the detergent effect in DDM-bound Wzz protein can be explained as follows. First, less detergent (DDM) is required to form the DDM-bound Wzz complex compared to the amount of detergents applied in the reports of many membrane-bound proteins. Second, DDM-bound Wzz protein is fairly elongated in solution (described below), rather than densely compact as revealed in some proteins like the peripheral light harvesting LH2 complex (*30*), and could make the existence of the surrounding monolayer detergent molecules less visible.

The Repulsive Interactions Possibly Occur among Wzz Molecules. To investigate whether concentration-dependent aggregation and the type of the intermolecular interactions take place among Wzz molecules, concentration-series studies by SAXS were performed. Further, as lower concentrations of samples are used in previous biochemical studies of Wzz (<0.2 mg/mL), it is necessary to investigate whether the protein remains to be a tetramer in SAXS and other structural studies, where higher concentrations of samples are often required. Thus the structural and biochemical studies can be properly compared. The concentration series studies (Figure 3) demonstrate that the SAXS patterns with different concentrations of DDM-bound Wzz protein are superimposable after scaling by concentration, except that the deviation is observed in very low Q-range ($Q < 0.02$ Å^{-1}, shown in Figure 3B), and the value of R_g decreases as concentration increases (Table 1). This result suggests that no concentration-dependent aggregations but most likely repulsive intermolecular interactions occur between Wzz molecules as the protein concentration increases. It is also possible that concentration-dependent conformational changes also correlate to the deviation of SAXS patterns in the very low Q-range and smaller R_g, even though several SAXS studies (*16*, *28*) indicate that the global conformational changes generally lead to deviation of the SAXS pattern in as well as beyond very low Q-range.

The molecular mechanisms that led to the proposed repulsion interaction, whether it results from the interactions of micelle or/and protein moiety of the DDM-bound Wzz proteins, remains to be investigated. The observation, nevertheless, provides one of the possible explanations for the lack of success in obtaining good crystals, since situations where intermolecular potentials are repulsive or strongly attractive do not generally lead to good crystal formation (*31*). As more and more membrane proteins are expected to

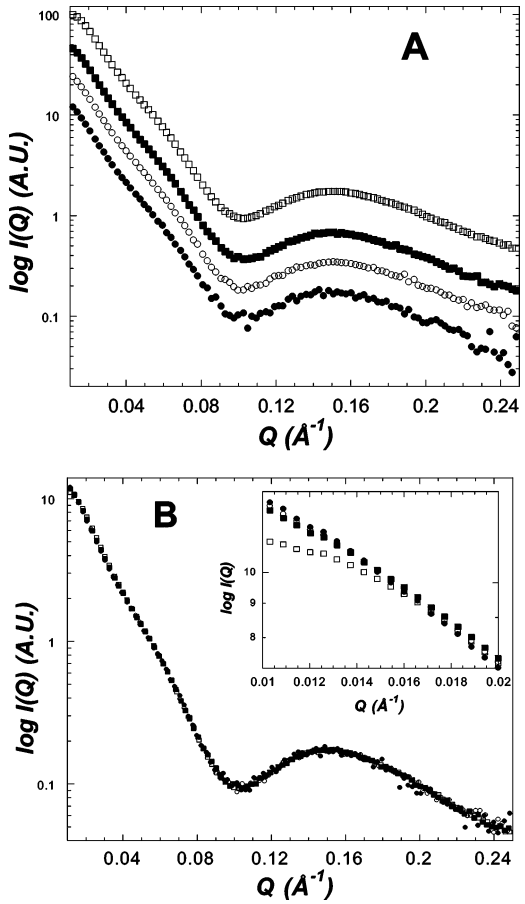

FIGURE 3: The concentration series measurements for DDM-bound Wzz (A); the data after scaling by concentration (B). The low Q data in (B) are shown in (B inset). The DDM-bound Wzz concentrations are 1 (●), 2 (○), 4 (■), and 10 (□) mg/mL, and the scattering intensity of buffer and DDM is subtracted.

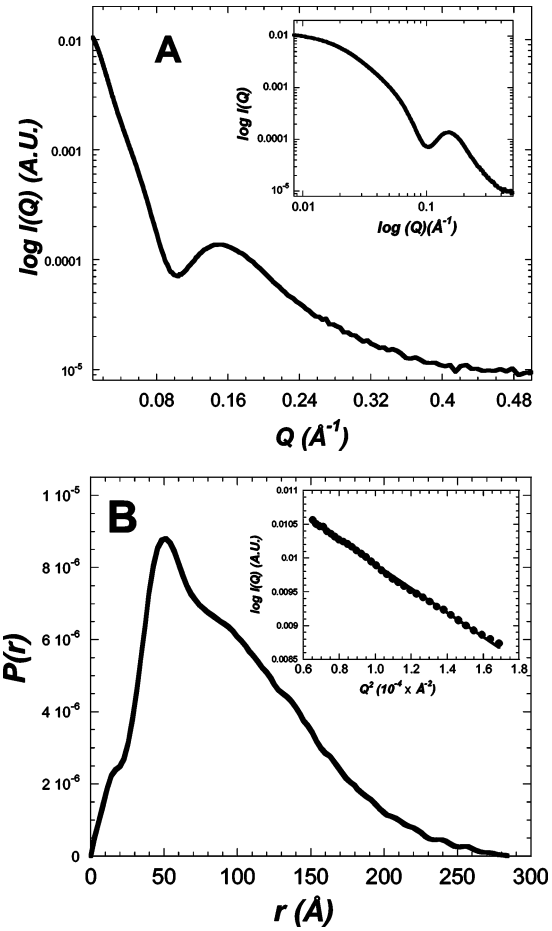

FIGURE 4: Characterization of DDM-bound Wzz by SAXS with 0.5 mg/mL Wzz in 20 mM Tris-HCl buffer at pH 8.0 and 0.05% DDM. The SAXS data are plotted in log $I(Q)$ vs Q (A) and in log $I(Q)$ vs log Q (A inset). The $P(r)$ and Guinier plots for SAXS data in (A) are shown in (B) and (B inset), respectively.

be investigated by small-angle X-ray/neutron scattering and other structural/biophysical methods, it is interesting to see whether the intermolecular interactions, particular repulsion interactions, may be detected in other transmembrane-associated proteins, and whether the intermolecular interactions may be functionally relevant.

Ionic Strength Effect Investigation. In addition to investigating the intermolecular interactions, we also examined the ionic strength effect for Wzz by SAXS. For many proteins with attractive intermolecular interactions, high salt concentration can minimize the aggregation and nonspecific interactions. No aggregation but rather intermolecular repulsion interactions are observed for Wzz in the absence of salt, whereas including 0.1 N NaCl in the solution leads to formation of oligomers larger than a tetramer. The value of R_g for Wzz protein increases from ~76 Å (in the absence of NaCl) to 100 Å or larger (in the presence of 0.1 N NaCl), and the forward scattering intensity ($I(0)$), which is largely determined by the molecular mass of the macromolecules, increases more than 2-fold for Wzz in 0.1 N NaCl. The sign of aggregation is reduced as NaCl concentration decreases. In another study, the Wzc oligomer complexes, larger than a tetrameric species, were detected over a wide range of protein concentrations (0.05−0.6 mg/mL) in 0.1 N NaCl (*15*), and similar results were also acquired in our SAXS studies of Wzz, where the aggregation in 0.1 N NaCl was observed in 0.25−16 mg/mL Wzz. While it remains to be further investigated whether the aggregation of Wzz is related to the presence of NaCl, we are currently investigating the possible physiological roles of NaCl on Wzz.

Table 2: SAXS Data for Wzz and the Wzz·O-Antigen Complex Obtained from Guinier Analyses and GNOM Fit

sample[a]	R_g Guinier	R_g GNOM	D_{max} (GNOM)
Wzz	76.2 ± 0.2	75.2 ± 0.2	275 ± 5
Wzz + 0.12 mg/mL O-antigen	75.2 ± 0.2	74.0 ± 0.4	270 ± 5
Wzz + 1.2 mg/mL O-antigen	70.1 ± 0.2	70.2 ± 0.3	255 ± 4
Wzz + 12 mg/mL O-antigen	66.0 ± 0.3	67.4 ± 0.4	233 ± 2

[a] 2 mg/mL of DDM-bound Wzz and 10−18 O units of O-antigen were used.

The Molecular Shape of DDM-Bound Wzz. The SAXS data analyses suggest that DDM-bound Wzz protein has an elongated particle shape based on the following evidence: (1) the curve shape of the $P(r)$ (the particle distance distribution function) plot (Figure 4); (2) the ratio of D_{max}/R_g: the ratio is ~3.8 for DDM-bound Wzz, in which the values of R_g and D_{max} are 76 ± 0.1 Å, and 275 ± 3 Å, respectively (Table 2), whereas the D_{max}/R_g ratio is ≤2.7−2.8 for a globular shape protein (*16*); and (3) the low resolution reconstructed model (Figure 5). The methods for acquiring R_g, D_{max}, $P(r)$ plot, and the reconstructed model are described in Materials and Methods.

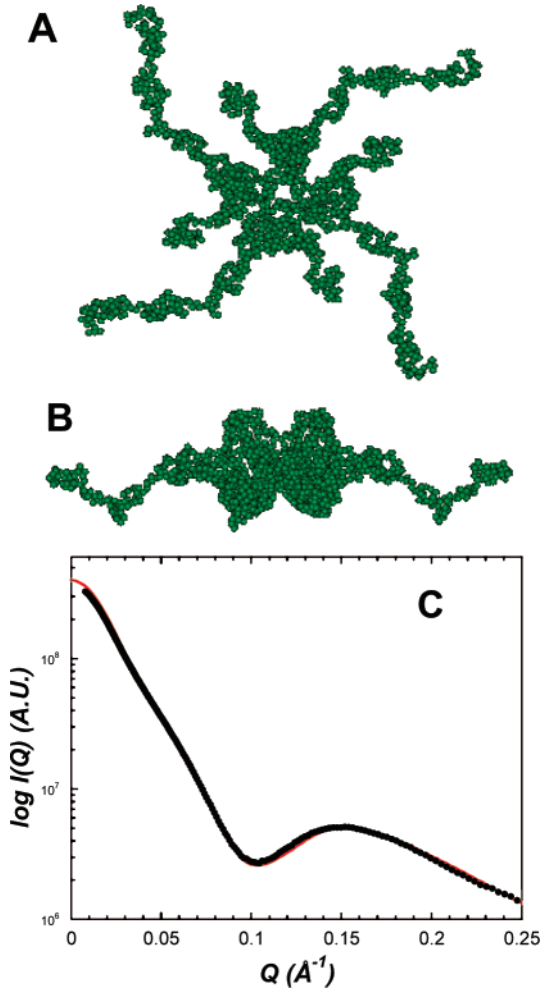

FIGURE 5: The low resolution reconstructed model constructed for DDM-bound Wzz. The top (A) and side (B) views of the represented *ab initio* model. The predicted SAXS pattern (red curve) calculated from the reconstructed model is fitted to the experimental SAXS data (●) (C).

Low Resolution Structures of Wzz. To provide further structural insights for Wzz, we employed the modeling program GASBOR to acquire low resolution models from SAXS data. Fifteen independent reconstruction runs were taken for every model shown in this report. The program DAMAVER (*27*), which aligns all probable reconstructed models and removes outlier models below a given cutoff volume, was used to generate the averaged model and the most possible model in Figure 5. Top and side views for the model are shown in Figures 5A and 5B, respectively. Other reconstructed models we generated are shown in Figure S1. To evaluate the quality of the *ab initio* model, we generate the predicted SAXS curves calculated from the reconstructed model by the program CRYSOL (*32*), and the predicted SAXS pattern fits very well with the experimental SAXS data (Figure 5C).

The reconstructed model can be compared to the proposed topology of Wzz (Figure 6). The reconstructed model suggests that the Wzz monomer interacts with other monomers at the middle region (Figure 5), likely representing the periplasmic domain in the proposed topology of Wzz (Figure 6). Similar results were also suggested by the cryo-EM studies of Wzc (*15*). Further, the biochemical *in vivo* studies in Wang's laboratory demonstrated that a predicted coiled-

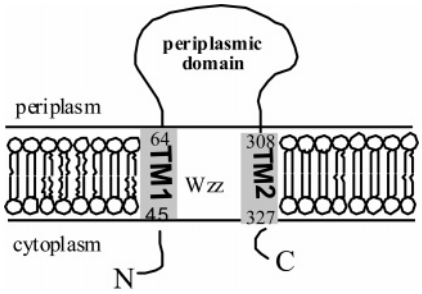

FIGURE 6: The possible topology of Wzz protein.

coil region (*13*) in the periplasmic domain can interact with the whole length of Wzz protein (see the later section). The oligomerization has been linked to the function of Wzz by mutagenesis studies (*33*). It needs to be noted that our low resolution model does not rule out possible interactions from other regions of Wzz, for example, TM1 and TM2 domains (Figure 6), that may also contribute to the tetramer formation.

Despite many similarities between DDM-bound Wzz and Wzc proteins being described in previous and current studies, the sequences of these two proteins are rather distinct. One of the intrinsic differences between these two proteins is that Wzc contains an extra C-terminal cytoplasmic domain (276 amino acid residues) harboring an ATP-binding motif and a tyrosine-rich motif, whereas only 10 amino acid residues are presented in the cytosolic C-terminus of Wzz (see Figure 6) and no studies on either N- or C-terminus of Wzz have yet been reported. Additionally, the phosphorylation of the tyrosine motif is essential for high level polymerization of Wzc protein (*15*). Together, the extended C-terminus of Wzc protein may partially explain the closed conformation of Wzc in cryo-EM studies, while the shorter C-terminus leads to more elongated shape of Wzz. Further, as illustrated in the studies described further below, Wzz appears to exist in an open conformation in the apo-form, and becomes more closed when the substrate (O-antigen) binds. Thus, it could be of functional importance for apo-Wzz being in the open and more flexible conformation. Although one may always consider that the differences in sample preparations and experimental conditions between cryo-EM and SAXS can possibly contribute to the conformational differences between these two proteins, several recent studies (*34*−*37*) demonstrated that similar structural information can be acquired by cryo-EM and solution SAXS studies. Together, the previous studies and this report suggest that Wzc and Wzz share similar functions with somewhat different sequences and structures/conformations.

Formation of Larger Wzz Oligomers. In our hands, the formation of Wzz oligomers larger than the identified tetramer has been frequently observed during SAXS measurements when the salt concentration or other reaction condition is varied. It is consistent with *in vivo* chemical cross-linking studies (*13*, *33*), where oligomeric complexes larger than a hexamer are detected in Wzz from *Shigella fexneri* (*33*) and from *E. coli* O86:H2 strain (*13*). Similarly, high molecular weight oligomers, larger than a tetramer, are also detected in Wzc protein (*15*). The formation of larger oligomers, however, could potentially play a role inregulating the length of polysaccharide. The discussion for this is presented in the next paragraph.

The Coiled-Coil Region Mediates Wzz Oligomerization. Wzz involved in LPS O-polysaccharide biosynthesis is

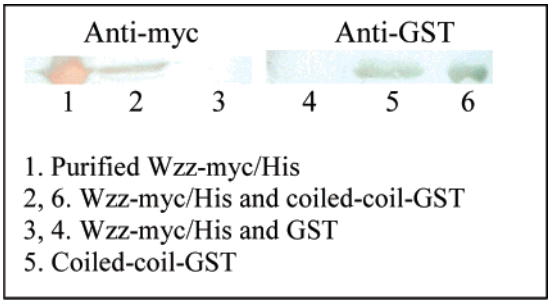

FIGURE 7: The interactions of coiled-coil truncated form and full-length Wzz investigated by Western immunoblotting analyses. The results indicate that the coiled-coil region interacts with the whole Wzz protein and could be the binding motif for the oligomerization of Wzz.

generally grouped into a "polysaccharide co-polymerase (PCP)" family (*38*). Most PCP proteins have a large periplasmic domain flanked by two transmembrane segments at N- and C-termini, respectively. It was previously reported that when the COILS program was used to analyze the periplasmic domain of the PCP proteins, many of them are likely to form coiled-coil motif (*39*). Further, the probability of coiled-coil formation, location and number of the coiled-coil motifs correlate with the degree of polymerization of the polysaccharide. Thus the coiled-coil motif has been proposed to play an important role in LPS modality determination and possibly the mediation of Wzz oligomerization. Here, we use pulldown assays to investigate whether the predicted coiled-coil region (residues 153−213) of Wzz is responsible for the oligomerization. Shown in Figure 7 is that the eluted protein sample has both anti-myc and anti-GST staining, suggesting the interaction between GST/coiled-coil and full-length Wzz. As a control, if only GST was expressed, no interaction was detected between Wzz and GST, indicating that the interaction between coiled-coil region and full-length Wzz is specific. Further, our preliminary CD and NMR studies suggested that the truncated Wzz protein (residues 153−213, without GST-fusion protein attached) may not be appropriately folded, and that the full length Wzz may function as a molecular chaperone that assists the truncated Wzz in folding. Together, our studies conclusively illustrate that the predicted coiled-coil region is at least partially responsible for the Wzz oligomerization. As oligomerization is important for the function of Wzz, we speculate that the oligomerization state of Wzz may correlate with the degree of polymerization carried out by Wzy (O-antigen polymerase).

SAXS Studies on Wzz·O-Antigen Complex. Wzz is functioning as an O-antigen chain length determinant protein (*1*), and can recognize different O-antigen chain length by changing specific amino acid substitutions in Wzz (*40*). It is of great interest to understand how Wzz can achieve this important biological function. Previous CD studies (*13*) indicated significant changes in the secondary structure of the intermediate form of Wzz upon the substrate (O-antigen) binding, raising the possibility that the CD spectral changes could reflect the possible substrate-induced conformational changes of Wzz. Herein, we report the SAXS measurements to test this hypothesis, as it is beyond the scope of the previous cryo-EM studies of Wzc (*15*). In the reaction of 2.0 mg/mL Wzz and O-antigen, as O-antigen concentration increases, the values of R_g and D_{max} decrease from 76 to 65

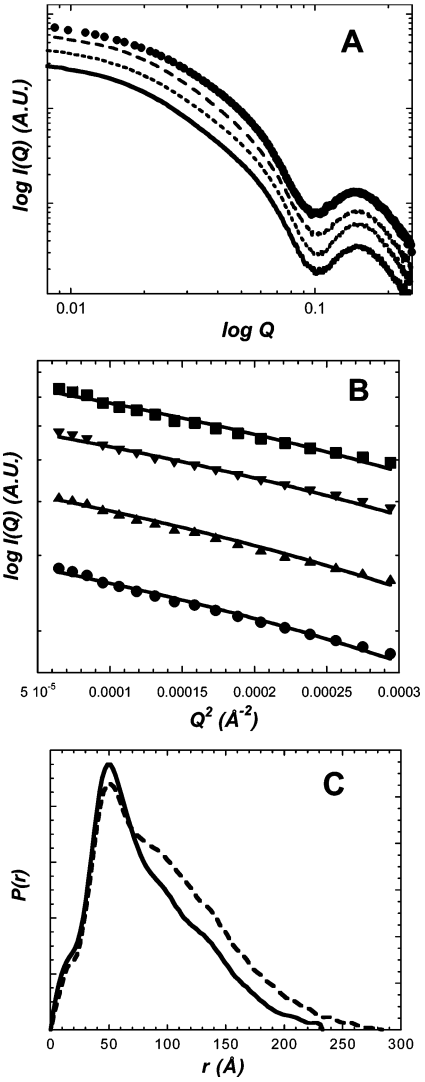

FIGURE 8: The reaction of Wzz and O-antigen investigated by SAXS. O-antigen titration to DDM-bound Wzz protein (2 mg/mL, 12 μM) is shown in (A), where the data are plotted in log $I(Q)$ vs log Q and shifted along the y-axis for comparison. The scattering signal of unbound O-antigen is subtracted from the SAXS pattern. The SAXS pattern of Wzz (represents DDM-bound Wzz) (—), Wzz + 0.12 mg/mL O-antigen (- - -), Wzz + 1.2 mg/mL O-antigen (— — —), and Wzz + 12 mg/mL O-antigen (●) are shown from bottom to top. The Guinier plots for Wzz (●), Wzz + 0.12 mg/mL O-antigen (▲), Wzz + 1.2 mg/mL O-antigen (▼), and Wzz + 12 mg/mL O-antigen (■) are shown in (B). The data are shifted along the y-axis for comparison. The $P(r)$ plot for Wzz (dashed line) and the Wzz·O-antigen complex (Wzz + 12 mg/mL O-antigen) (solid line) is shown in (C).

Å and from 275 to 233 Å, respectively (Figure 8 and Table 2), indicating that the Wzz·O-antigen complex is more compact than Wzz protein. The overall shapes of Wzz and the Wzz·O-antigen complex likely remain to be similar, as the ratio of D_{max}/R_g is unchanged for Wzz (3.6) and the Wzz·O-antigen complex (3.5). Also, the $I(0)$ slightly increases for the Wzz·O-antigen complex, which is expected as the mass is much larger for DDM-bound Wzz (∼224 kDa (*13*) or ∼256 kDa estimated herein) than for O-antigen (13−24 kDa). Together, the SAXS studies indicate possible substrate-induced conformational changes, consistent with the secondary structure changes indicated by previous CD data (*13*).

How Wzz Regulates the Chain Length of O-Antigen. The possible conformational change described above may not

only lead to stronger interactions between Wzz and O-antigen but also correlate to the biological function of Wzz, in which a more compact Wzz−O-antigen complex could be required to terminate the polymerization and regulate the length of O-antigen. As described in the introduction, two models have been proposed for the Wzz biological function: either Wzz behaves like a timing clock that interacts with Wzy and regulate Wzy activity (*11*) or it works as a molecular chaperone that interacts with Wzy, WaaL, and nascent polysaccharide chains (*12*), yet not enough evidence is available for either model. Together with the Wzz−Wzy interactions suggested by the work in Wang's laboratory (data not shown), our present studies, in which (the full-length) Wzz directly interacts with O-antigen and may assist the truncated (residues 153−213) Wzz protein in folding, do not support the molecular timer (timing clock) model. Rather, our data are consistent with the molecular chaperone model (*12*), and provide the biochemical and structural evidence for the proposed interactions between polysaccharide and Wzz in the model.

Conclusions/Remarks. Wzz and Wzc, the other membrane-associated protein, have similar physiological functions despite low homology (10.7% identity and 19.3% similarity). The low resolution structure of Wzc was characterized as a tetramer by cryo-EM (*15*), and our present studies also indicate that Wzz appears to be a tetramer and the oligomerization site is also in the middle region of Wzz, which is likely to be located in the periplasmic domain. Moreover, our studies show that O-antigen interacts directly with Wzz and induces possible substrate-induced conformational changes of Wzz, suggesting a possible molecular mechanism for Wzz to regulate the O-antigen chain length in the Wzy-dependent pathway.

ACKNOWLEDGMENT

The SAXS experiments were conducted at BL 4-2 of the Stanford Synchrotron Radiation Laboratory (SSRL) and BioCAT 18-ID of the Advanced Photon Source (APS), supported by the National Institutes of Health and the Department of Energy. K.-H.T. thanks Dr. Marc Niebuhr (SSRL) and Dr. Liang Guo (APS) for the assistance on SAXS beam line and data collection.

SUPPORTING INFORMATION AVAILABLE

Other represented reconstructed models for Wzz proteins generated by modeling program (Figure S1). This material is available free of charge via the Internet at http://pubs.acs.org.

REFERENCES

1. Raetz, C. R., and Whitfield, C. (2002) Lipopolysaccharide endotoxins, *Annu. Rev. Biochem. 71*, 635−700.
2. Najdenski, H., Golkocheva, E., Vesselinova, A., Bengoechea, J. A., and Skurnik, M. (2003) Proper expression of the O-antigen of lipopolysaccharide is essential for the virulence of Yersinia enterocolitica O:8 in experimental oral infection of rabbits, *FEMS Immunol. Med. Microbiol. 38*, 97−106.
3. Burrows, L. L., Chow, D., and Lam, J. S. (1997) Pseudomonas aeruginosa B-band O-antigen chain length is modulated by Wzz (Ro1), *J. Bacteriol. 179*, 1482−1489.
4. Marolda, C. L., Vicarioli, J., and Valvano, M. A. (2004) Wzx proteins involved in biosynthesis of O antigen function in association with the first sugar of the O-specific lipopolysaccharide subunit, *Microbiology 150*, 4095−4105.
5. Feldman, M. F., Marolda, C. L., Monteiro, M. A., Perry, M. B., Parodi, A. J., and Valvano, M. A. (1999) The activity of a putative polyisoprenol-linked sugar translocase (Wzx) involved in Escherichia coli O antigen assembly is independent of the chemical structure of the O repeat, *J. Biol. Chem. 274*, 35129−35138.
6. Liu, D., Cole, R. A., and Reeves, P. R. (1996) An O-antigen processing function for Wzx (RfbX): a promising candidate for O-unit flippase, *J. Bacteriol. 178*, 2102−2107.
7. Grozdanov, L., Zahringer, U., Blum-Oehler, G., Brade, L., Henne, A., Knirel, Y. A., Schombel, U., Schulze, J., Sonnenborn, U., Gottschalk, G., Hacker, J., Rietschel, E. T., and Dobrindt, U. (2002) A single nucleotide exchange in the wzy gene is responsible for the semirough O6 lipopolysaccharide phenotype and serum sensitivity of Escherichia coli strain Nissle 1917, *J. Bacteriol. 184*, 5912−5925.
8. Bengoechea, J. A., Pinta, E., Salminen, T., Oertelt, C., Holst, O., Radziejewska-Lebrecht, J., Piotrowska-Seget, Z., Venho, R., and Skurnik, M. (2002) Functional characterization of Gne (UDP-N-acetylglucosamine-4-epimerase), Wzz (chain length determinant), and Wzy (O-antigen polymerase) of Yersinia enterocolitica serotype O:8, *J. Bacteriol. 184*, 4277−4287.
9. Daniels, C., Vindurampulle, C., and Morona, R. (1998) Overexpression and topology of the Shigella flexneri O-antigen polymerase (Rfc/Wzy), *Mol. Microbiol. 28*, 1211−1222.
10. Wu, T., McCandlish, A. C., Gronenberg, L. S., Chng, S. S., Silhavy, T. J., and Kahne, D. (2006) Identification of a protein complex that assembles lipopolysaccharide in the outer membrane of Escherichia coli, *Proc. Natl. Acad. Sci. U.S.A. 103*, 11754−11759.
11. Bastin, D. A., Stevenson, G., Brown, P. K., Haase, A., and Reeves, P. R. (1993) Repeat unit polysaccharides of bacteria: a model for polymerization resembling that of ribosomes and fatty acid synthetase, with a novel mechanism for determining chain length, *Mol. Microbiol. 7*, 725−734.
12. Morona, R., van den Bosch, L., and Manning, P. A. (1995) Molecular, genetic, and topological characterization of O-antigen chain length regulation in Shigella flexneri, *J. Bacteriol. 177*, 1059−1068.
13. Guo, H., Lokko, K., Zhang, Y., Yi, W., Wu, Z., and Wang, P. G. (2006) Overexpression and characterization of Wzz of Escherichia coli O86:H2, *Protein Expression Purif. 48*, 49−55.
14. Collins, R. F., Beis, K., Dong, C., Botting, C. H., McDonnell, C., Ford, R. C., Clarke, B. R., Whitfield, C., and Naismith, J. H. (2007) The 3D structure of a periplasm-spanning platform required for assembly of group 1 capsular polysaccharides in Escherichia coli, *Proc. Natl. Acad. Sci. U.S.A. 104*, 2390−2395.
15. Collins, R. F., Beis, K., Clarke, B. R., Ford, R. C., Hulley, M., Naismith, J. H., and Whitfield, C. (2006) Periplasmic protein-protein contacts in the inner membrane protein Wzc form a tetrameric complex required for the assembly of Escherichia coli group 1 capsules, *J. Biol. Chem. 281*, 2144−2150.
16. Vachette, P., Koch, M. H., and Svergun, D. I. (2003) Looking behind the beamstop: X-ray solution scattering studies of structure and conformational changes of biological macromolecules, *Methods Enzymol. 374*, 584−615.
17. Mylonas, E., and Svergun, D. I. (2007) Accuracy of molecular mass determination of proteins in solution by small-angle X-ray scattering, *J. Appl. Crystallogr. 40*, S245−S249.
18. Glatter, O., and Kratky, O. (1982) *Small-angle X-ray Scattering*, Academic Press, London.
19. O'Neill, H., Heller, W. T., Helton, K. E., Urban, V. S., and Greenbaum, E. (2007) Small-angle X-ray scattering study of photosystem I-detergent complexes: implications for membrane protein crystallization, *J. Phys. Chem. B 111*, 4211−4219.
20. Columbus, L., Lipfert, J., Klock, H., Millett, I., Doniach, S., and Lesley, S. A. (2006) Expression, purification, and characterization of Thermotoga maritima membrane proteins for structure determination, *Protein Sci. 15*, 961−975.
21. Strop, P., and Brunger, A. T. (2005) Refractive index-based determination of detergent concentration and its application to the study of membrane proteins, *Protein Sci. 14*, 2207−2211.
22. VanAken, T., Foxall-VanAken, S., Castleman, S., and Ferguson-Miller, S. (1986) Alkyl glycoside detergents: synthesis and applications to the study of membrane proteins, *Methods Enzymol. 125*, 27−35.
23. Svergun, D. I. (1992) Determination of the regularization parameter in indirect-transform methods using perceptual criteria, *J. Appl. Crystallogr. 25*, 495−503.

24. Guinier, A., and Fournet, G. (1955) *Small-Angle Scattering of X-Rays*, John Wiley & Sons, Inc., New York.
25. Svergun, D. I., Petoukhov, M. V., and Koch, M. H. (2001) Determination of domain structure of proteins from X-ray solution scattering, *Biophys. J. 80*, 2946−2953.
26. Konarev, P. V., Volkov, V. V., Sokolova, A. V., Koch, M. H. J., and Svergun, D. I. (2003) PRIMUS: a windows PC-based system for small-angle scattering data analysis, *J. Appl. Crystallogr. 36*, 1277−1282.
27. Volkov, V. V., and Svergun, D. I. (2003) Uniqueness of *ab initio* shape determination in small-angle scattering, *J. Appl. Crystallogr. 36*, 860−864.
28. Koch, M. H., Vachette, P., and Svergun, D. I. (2003) Small-angle scattering: a view on the properties, structures and structural changes of biological macromolecules in solution, *Q. Rev. Biophys. 36*, 147−227.
29. Hong, X., Weng, Y. X., and Li, M. (2004) Determination of the topological shape of integral membrane protein light-harvesting complex LH2 from photosynthetic bacteria in the detergent solution by small-angle X-ray scattering, *Biophys. J. 86*, 1082−1088.
30. Du, L.-C., Weng, Y. X., Hong, X., Xian, D.-C., and Kobayashi, K. (2006) Synchrotron small-angle x-ray scattering investigation on integral membrane protein light-harvesting complex LH2 from photosynthetic bacterium *Rhodopseudomonas Acidophila*, *Chin. Phys. Lett. 23*, 1861−1863.
31. Hitscherich, C., Aseyev, V., Wiencek, J., and Loll, P. J. Jr. (2001) Effects of PEG on detergent micelles: implications for the crystallization of integral membrane proteins, *Acta Crystallogr., Sect. D: Biol. Crystallogr. 57*, 1020−1029.
32. Svergun, D. I., Barberato, C., and Koch, M. H. J. (1995) CRYSOL - a program to Evaluate X-ray Solution Scattering of Biological Macromolecules from Atomic Coordinates, *J. Appl. Crystallogr. 28*, 768−773.
33. Daniels, C., and Morona, R. (1999) Analysis of Shigella flexneri wzz (Rol) function by mutagenesis and cross-linking: wzz is able to oligomerize, *Mol. Microbiol. 34*, 181−194.
34. Tidow, H., Melero, R., Mylonas, E., Freund, S. M., Grossmann, J. G., Carazo, J. M., Svergun, D. I., Valle, M., and Fersht, A. R. (2007) From the Cover: Quaternary structures of tumor suppressor p53 and a specific p53 DNA complex, *Proc. Natl. Acad. Sci. U.S.A. 104*, 12324−12329.
35. Redecke, L., von Bergen, M., Clos, J., Konarev, P. V., Svergun, D. I., Fittschen, U. E., Broekaert, J. A., Bruns, O., Georgieva, D., Mandelkow, E., Genov, N., and Betzel, C. (2007) Structural characterization of beta-sheeted oligomers formed on the pathway of oxidative prion protein aggregation in vitro, *J. Struct. Biol. 157*, 308−320.
36. Sokolova, A. V., Kreplak, L., Wedig, T., Mucke, N., Svergun, D. I., Herrmann, H., Aebi, U., and Strelkov, S. V. (2006) Monitoring intermediate filament assembly by small-angle x-ray scattering reveals the molecular architecture of assembly intermediates, *Proc. Natl. Acad. Sci. U.S.A. 103*, 16206−16211.
37. Gherardi, E., Sandin, S., Petoukhov, M. V., Finch, J., Youles, M. E., Ofverstedt, L. G., Miguel, R. N., Blundell, T. L., Vande Woude, G. F., Skoglund, U., and Svergun, D. I. (2006) Structural basis of hepatocyte growth factor/scatter factor and MET signalling, *Proc. Natl. Acad. Sci. U.S.A. 103*, 4046−4051.
38. Morona, R., Van Den Bosch, L., and Daniels, C. (2000) Evaluation of Wzz/MPA1/MPA2 proteins based on the presence of coiled-coil regions, *Microbiology 146*, 1−4.
39. Lupas, A. (1996) Prediction and analysis of coiled-coil structures, *Methods Enzymol. 266*, 513−525.
40. Franco, A. V., Liu, D., and Reeves, P. R. (1998) The wzz (cld) protein in Escherichia coli: amino acid sequence variation determines O-antigen chain length specificity, *J. Bacteriol. 180*, 2670−2675.

BI701181R